Available online at www.sciencedirect.com
ScienceDirect
Atmospheric Environment 42 (2008) 1461–1475
ATMOSPHERIC ENVIRONMENT
www.elsevier.com/locate/atmosenv

Impact of transport of sulfur dioxide from the Asian continent on the air quality over Korea during May 2005

Chulkyu Lee[a,*], Andreas Richter[a], Hanlim Lee[b], Young J. Kim[b], John P. Burrows[a], Young G. Lee[c], Byeong C. Choi[c]

[a]*Institute of Environmental Physics and Remote Sensing, University of Bremen, Otto-Hahn-Allee 1, D-28334 Bremen, Germany*
[b]*Advanced Environmental Monitoring Research Center, Gwangju Institute of Science and Technology, 1 Oryong-dong, Buk-gu, Gwangju 500-712, Republic of Korea*
[c]*Meteorological Research Institute, 460-18 Sindaebang-dong, Dongjak-gu, Seoul 156-720, Republic of Korea*

Received 18 May 2007; received in revised form 31 October 2007; accepted 5 November 2007

Abstract

The East Asian countries have been affected by atmospheric gaseous pollutants (in particular SO_2) transported from the Asian continent as well as Asian dust storms. For investigation of the impact of these anthropogenic trace gases on local air quality in Korea, ground-based measurements using a Multi-Axis Differential Optical Absorption Spectroscopy (MAX-DOAS) system and in situ gas analyzers as well as synoptic meteorological data and scattered sunlight spectra obtained by the satellite-borne instrument, Scanning Imaging Absorption Spectrometer for Atmospheric Chartography (SCIAMACHY) launched on board of Environmental Satellite (ENVISAT) in March 2002, were utilized to retrieve SO_2 and trace its transport from the Asian continent to Korea in May 2005. The ground-based measurements were carried out in the region of interest, at Korea Global Watch Observatory (KGAWO) in Korea. Plumes of high SO_2 over Chinese industrial areas and their transport to the Korean peninsula were observed in SCIAMACHY data in the period of 21–26 May 2005. Highly increased SO_2 was measured by the MAX-DOAS system and in situ gas analyzer in the period of 27–29 May 2005 at KGAWO. These observations are supported by the meteorological results that the air-masses picking up these high SO_2 plumes while passing over the Chinese industrial and metropolitan areas were transported to the Korean peninsula. The tropospheric SO_2 VCDs over these Chinese industrial and metropolitan areas ranged up to 1.4×10^{17} mol cm^{-2} in SCIAMACHY data. These SO_2 plumes resulted in increased SO_2 surface levels of up to 7.8 ppbv (measured by an in situ gas analyzer) at KGAWO.

Keywords: Anthropogenic SO_2; Air pollutant transport; UV spectroscopy; DOAS

1. Introduction

Anthropogenic emissions of atmospheric pollutants in East Asian countries are of great concern because of their impact on the atmospheric environment on regional and intercontinental scales. The East Asian countries have been affected by atmospheric gaseous pollutants (in particular SO_2) transported from the Asian continent as well as Asian dust storms containing a toxic mixture of heavy metals and carcinogens accumulated as the

*Corresponding author.
E-mail address: cklee79@gmail.com (C. Lee).

1352-2310/$ - see front matter © 2007 Elsevier Ltd. All rights reserved.
doi:10.1016/j.atmosenv.2007.11.006

clouds pass over Chinese industrial areas (Koike et al., 2003; Zhang et al., 2003; Tu et al., 2004; Jaffe et al., 2005). Rapid economic growth and increasing fossil fuel energy consumption in China in the past decades has resulted in large emissions of reactive sulfur compounds into the atmosphere.

Sulfur dioxide (SO_2) is an important trace species in the atmosphere, both under background conditions and in polluted areas (Chin and Jacob, 1996; Berglen et al., 2004). It is released into the troposphere as a result of anthropogenic and natural phenomena. The SO_2 emitted is chemically converted to sulfuric acids in the atmosphere both in the gaseous and aqueous phases (Chin and Jacob, 1996). When these acids precipitate, damage is caused to ecosystems and buildings. Related formation of sulfuric acid (sulfate) aerosols can cause human respiratory morbidity and mortality. Sulfate aerosols have a cooling effect on the Earth's surface (Intergovernmental Panel on Climate Change (IPCC), 2001). These sulfate particles reflect energy coming from the sun, thereby decreasing the amount of sunlight reaching and heating the Earth's surface. Myhre et al. (2004) suggested that most of the lower stratospheric sulfate aerosol is of anthropogenic origin and a global mean radiative forcing due to the anthropogenic influence on the stratospheric aerosol layer results in $-0.05\,W\,m^{-2}$. This represents a new climate forcing mechanism and emphasizes anthropogenic sulfur emission as an important cooling mechanism (Myhre et al., 2004).

Anthropogenic emissions of SO_2 occur predominantly at the continental surface and chemical conversion and loss processes take place during transport. Air pollutants are transported in the atmosphere via advection and turbulent diffusion processes. Their concentrations in the free troposphere are usually lower than those in the boundary layer, because a large fraction of the species remains within boundary layer and a small fraction of them is transported to the free troposphere. Those airmasses uplifted from the source region are transported to the Korean peninsula by prevailing westerly wind increasing with altitude (Koike et al., 2003). Processes of transport and the regional budget of anthropogenic nitrogen and sulfur compounds over the East Asia region have been investigated using model simulations and aircraft measurements (Chin et al., 2000; Tan et al., 2002; Koike et al., 2003; Stohl et al., 2003; Guttikunda et al., 2005).

Since the 1970s, Differential Optical Absorption Spectroscopy (DOAS) has been used as a powerful tool for the detection of atmospheric trace species on a real-time basis (Platt, 1994). Using the DOAS technique, a number of atmospheric trace gases can be retrieved from the UV and visible region of the spectra, including O_3, NO_2, BrO, OClO, SO_2, HCHO, CHOCHO, and H_2O (Hausmann and Platt, 1994; Hebestreit et al., 1999; Afe et al., 2004; Wittrock et al., 2006). The Multi-Axis Differential Optical Absorption Spectroscopy (MAX-DOAS) technique is a passive DOAS technique using scattered sunlight from several viewing directions in addition to conventional zenith pointing. The measurements using low-viewing angles emphasize the absorption path in the lowermost atmospheric layers and the sensitivity for absorbers in the boundary layer is strongly enhanced, while the photons received from the zenith-looking telescope have traveled a relatively long path in the stratosphere and a comparatively short path in the troposphere (Hönninger et al., 2004). A MAX-DOAS system using a single telescope for receiving the scattered sunlight was used to investigate local air quality in this work. Satellite remote sensing techniques, in particular using the DOAS technique, have been employed for the measurement of atmospheric trace species on global and regional scales (e.g., Wagner and Platt, 1998; Palmer et al., 2003; Richter et al., 2005; Wittrock et al., 2006). The SCIAMACHY (Scanning Imaging Absorption Spectrometer For Atmospheric Chartography, http://www.iup.uni-bremen.de/sciamachy/), satellite instrument launched on board of ENVISAT in March 2002 (Bovensmann et al., 1999), performs continuous measurements of transmitted, reflected and scattered sunlight in the ultraviolet, visible, and shortwave infrared wavelength region. The radiance measurements contain information on concentration and distribution of atmospheric trace gases showing spectral absorption features in the absorbed wavelength interval (Bovensmann et al., 1999). Here, SCIAMACHY measurements in the nadir (down-looking) mode were utilized to retrieve SO_2 and to trace its transport from the Asian continent to East Asian countries.

The objective of this work was to investigate the impact of atmospheric trace gases (mainly SO_2) transported from the Asian continent on air quality over Korea. To achieve this objective, the

following scientific questions were addressed in this study:

(1) What is the extent of long-range transport of anthropogenic trace gases (e.g., SO_2) from the Asian continent?
(2) What is the impact of these atmospheric trace gases on local air quality over Korea?

More specifically, ground-based and satellite measurement data as well as meteorological data have been utilized to investigate the impact of the anthropogenic trace gases transported from the Asian continent in May 2005 over Korea.

2. Data set

The data sets used in this work include MAX-DOAS data, in situ air-quality monitoring data, SCIAMACHY Level 1 data, and global grid final run (FNL) meteorological data. Ground-based measurements using a MAX-DOAS system (NO_2 and SO_2) and in situ analyzers for NO_x (ML9841A, Teledyne Instruments), SO_2 (ML9850, Teledyne Instruments), CO (ML9830, Teledyne Instruments), O_3 (ML9812, Teledyne Instruments), and PM_{10} (β-ray PM_{10}, FH62C14, Thermo Andersen) were carried out to obtain local air-quality data in the region of interest from 20 May to 9 June 2005, at the Korea Global Atmosphere Watch Observatory (KGAWO) (36.56°N, 127.47°E) located on Anmyeon Island off the west coast of Korea.

2.1. Ground-based MAX-DOAS data

Our sequential MAX-DOAS system mainly consists of a small aluminum box containing a miniature spectrograph and a telescope. The miniature spectrograph (OceanOptics USB2000, cross Czerny-Turner type, $1/f = 4$) consists of a grating (2400 grooves mm^{-1}) yielding spectral coverage between 289 and 431 nm (at 0.7 nm FWHM spectral resolution) and a CCD detector (2048 pixels at 14 μm center-to-center spacing) (Lee et al., 2005b). The MAX-DOAS box was attached directly to a stepper motor, allowing sequential measurement of scattered sunlight at various elevation angles between 0° and 90° above the horizon. MAX-DOAS measurements were made from the roof of the KGAWO building (43 m above sea level) during daytime from 27 May to 9 June 2005 (UT). The viewing azimuth angle of the MAX-DOAS telescope was 340° (0° means true north direction), looking to the sea. Scattered sunlight signals were recorded at telescope elevation angles of 3°, 6°, 10°, 20°, and 90°. Each measurement sequence took about 10–20 min. Measured MAX-DOAS spectra were analyzed to identify and quantify levels of SO_2 and NO_2 using their specific structured absorption features in the ultraviolet region (Platt, 1994).

The spectra taken by the MAX-DOAS system were calibrated using mercury lamp line peaks corrected for dark current and electric offset signal by subtracting the dark current and offset signals recorded. Then the spectra were calibrated again by fitting them to a solar reference spectrum, and slant column densities (SCDs) of SO_2 and NO_2 were derived from the calibrated DOAS spectra using the WinDOAS V2.10 software package (Van Roozendael and Fayt, 2001). Scattered sunlight is highly structured due to solar Fraunhofer lines. Literature reference absorption cross-section spectra as well as the Fraunhofer Reference Spectrum (FRS) and Ring spectrum were simultaneously fitted to the scattered sunlight spectra using the nonlinear least-square method, in addition to a polynomial order fit to remove broad band structures (Stutz and Platt, 1996). A scattered sunlight spectrum taken at an elevation angle of 90° (zenith direction) around noon on (local time) of a cloudless day (30 May 2005) was used as the FRS, when only negligible background trace gas absorption was present. High-resolution reference absorption spectra were taken from the literatures (Greenblatt et al., 1990; Simon et al., 1990; Vandaele et al., 1997; Wilmouth et al., 1999; Bogumil et al., 2003). The Ring spectrum was calculated from the FRS (Bobrowski et al., 2003; Hönninger et al., 2004; Lee et al., 2005b). All reference absorption cross-section spectra were convoluted with the instrumental function to match the spectral resolution of the MAX-DOAS system used in this study. The specifications for the evaluation of SO_2 and NO_2 are summarized in Table 1. The fitting errors for the MAX-DOAS SO_2 and NO_2 were $<15\%$ and 7%, respectively. The retrieved SCDs from MAX-DOAS spectra recorded at a 90° elevation angle were subtracted from those obtained at other elevation angles during each scanning sequence. This procedure yielded differential SCDs (DSCDs) ($= \mathrm{SCD}(\alpha,\theta) - \mathrm{SCD}(90°,\theta)$), where α is the elevation angle and θ the solar zenith angle and removed absorptions by trace gases in the stratosphere (Leser et al., 2003).

Table 1
Specifications for the evaluation of MAX-DOAS and SCIAMACHY data

Data	Molecule	Wavelength range (nm)	Polynomial order	Cross-sections included in the fitting procedure
MAX-DOAS	SO_2	303.5–316	3	SO_2[a], NO_2[b], O_3[c], BrO[d], ClO[e], Ring[f], FRS[g]
	NO_2	399–418	3	NO_2[b], O_4[h], O_3[c], Ring[f], FRS[g]
SCIAMACHY	SO_2	315–327	4	SO_2[i], O_3[c], Ring[j], USamp[k], ETA[l]

The cross-sections of NO_2, O_3, and SO_2 for the evaluation of MAX-DOAS were I_0-corrected (Aliwell et al., 2002).
[a]SO_2 at 293 K (Bogumil et al., 2003).
[b]NO_2 at 294 K (Vandaele et al., 1997).
[c]Two O_3 cross-sections obtained at 223 and 243 K (Bogumil et al., 2003) were included in the fitting routine.
[d]BrO at 298 K (Wilmouth et al., 1999).
[e]ClO at 300 K (Simon et al., 1990).
[f]Ring spectrum.
[g]Fraunhofer Reference Spectrum.
[h]O_4 at 296 K (Greenblatt et al., 1990).
[i]SO_2 at 295 K (Vandaele et al., 1994).
[j]Ring spectrum (Vountas et al., 1998).
[k]Undersampling correction.
[l]Polarization dependency of the SCIAMACHY instrument.

2.2. Meteorological data

FNL data which uses the Global Spectral Medium-Range Forecast model to assimilate multiple sources of measured data and forecast meteorology are available from the National Oceanic and Atmospheric Administrations (NOAA) Air Resource Laboratory (ARL; ftp://www.arl.noaa.gov/pub/archives/fnl/). FNL data were used to estimate synoptic conditions over the study area and to calculate backward trajectories of air-masses with the Hybrid Single-Particle Lagrangian Integrated Trajectory (HYSPLIT-4; http://www.arl.noaa.gov/ready/hysplit4.html). The HYSPLIT-4 model was also used to characterize the transport pattern of air-mass flow over the study area. Vertical motions are calculated using the isentropic method with 5-day backward trajectory calculations (500, 1000, and 2000 m above the ground level). Moreover, local meteorological data that included wind speed and direction were also collected by an automatic weather station (AWS) installed 40 m above the ground level at KGAWO.

2.3. SCIAMACHY data

The SCIAMACHY is one of the instruments on board European Space Agency's (ESA) Environmental Satellite (ENVISAT) which was launched in a sun-synchronous orbit on 1 March 2002 and is in nominal operation since August 2002 (Bovensmann et al., 1999). The SCIAMACHY instrument is an eight channel grating spectrometer measuring light scattered by the Earth's atmosphere and surface in nadir, limb, and occultation (both solar and lunar) geometries. SCIAMACHY covers the spectral region from 220 to 2400 nm with a spectral resolution of 0.25 nm in the UV, 0.4 nm in the visible and less in the NIR. The size of the nadir ground-pixels depends on wavelength range and solar elevation and can be as small as $30 \times 30\,km^2$. In the above wavelength regions, several trace gases (e.g., BrO, NO_2, CHOCHO, HCHO, SO_2, OClO, O_3, etc.) have been detected (Eisinger and Burrows, 1998; Wagner and Platt, 1998; Afe et al., 2004; Buchwitz et al., 2005; Richter et al., 2005; Wittrock et al., 2006).

The SO_2 analysis for SCIAMACHY is based on the DOAS retrieval method (Eisinger and Burrows, 1998; Afe et al., 2004; Richter et al., 2006). The wavelength range of 315–327 nm was used for the SO_2 DOAS fit as the differential absorptions are large and interference by other species is small. In addition to the SO_2 cross-section (Vandaele et al., 1994), two ozone cross-sections (Bogumil et al., 2003), a synthetic Ring spectrum (Vountas et al., 1998), an undersampling correction (Chance, 1998), and the polarization dependency of the SCIAMACHY instrument are included in the fit (see Table 1). Daily solar irradiation measurements taken with the ASM diffuser are used as background spectrum. Most of fitting errors over East

Asia during the period of interest were <200%, and the data with fitting errors <150% were used in the following procedure. A latitude dependent offset was removed by subtracting the column taken on the same day at the same latitude in the 180–230° longitude region from the total column by the reference sector method (Richter and Burrows, 1999; Sierk et al., 2006). A cloud screening is applied to remove those measurements with a cloud fraction of >0.6 as determined from SCIAMACHY measurements using the SACURA algorithm (Kokhanovsky et al., 2006). Then the tropospheric slant column was converted to a vertical tropospheric column using an appropriate air-mass factor (AMF). The AMF is defined as the ratio of the observed slant column to the vertical column. It was calculated with a radiative transfer model, SCIATRAN (from Institute of Environmental Physics and Remote Sensing, University of Bremen, Germany), assuming full multiple scattering, surface albedo of 0.03, solar zenith angle of 40°, maritime (LOWTRAN) aerosol loading, and a SO_2 vertical profile which remains invariant from 0 to 1 km, decreases exponentially from 1 to 10 km and reaches drop down to zero above 11 km. The error induced from the AMF calculation by this assumption for boundary layer SO_2 was <20% (Eisinger and Burrows, 1998; Afe et al., 2004).

3. Results and discussion

3.1. Ground-based measurements

Fig. 1 shows the DSCDs and mixing ratios of atmospheric SO_2 and NO_2 measured by the MAX-DOAS system at KGWO located at Anmyeon from 27 May to 9 June 2005 (UT). The temporal variations of atmospheric NO_2, SO_2, PM_{10}, CO, NO, and O_3 concentrations measured by in situ monitors at KGWO from 21 May to 10 June 2005 (UT) are plotted in Fig. 2. Relatively high SO_2 and NO_2 levels were observed during two periods: 27–29 May (the first event period) and 4–7 June 2005 (the second event period). High SO_2 DSCDs observed by the MAX-DOAS system during the first period decreased to low values, and then they slightly got higher during the second period. The SO_2 trend determined by the MAX-DOAS system was not in agreement with that seen by the in situ gas analyzer during the first event period, unlike in the case of NO_2. Relatively high NO_2 DSCDs were observed during both periods. Relatively high PM_{10} concentrations were also observed during the first event period.

The discrepancy in SO_2 trends between the MAX-DOAS and in situ monitors during the first event period could be due to the inhomogeniety of air-masses. The major difference between the MAX-DOAS system and in situ instruments is that the passive MAX-DOAS system relies on the sun as its light source. Therefore, instrumental differences associated with measurement principles (i.e., line-integrating versus point measurement) need to be considered for an evaluation of MAX-DOAS performance (Lee et al., 2005a). The KGAWO site could be affected by the long-range transport of pollutants from the Asian continent. The air-mass transported from the Asian continent could be in the upper part of the boundary layer over the KGAWO site, and might have spread horizontally and towards the ground during the first event period. It is believed that the aged air-mass had an impact during the first event period. This is supported by HYSPLIT-4 modeling results indicating the air-mass transport from Asian continent (to be discussed in Section 3.2), satellite SO_2 images (to be discussed in Section 3.3), and high SO_4^{2-}/SO_2 ratios of PM_1 samples collected by an URG PM_1 sampler as summarized in Table 2. The MAX-DOAS system could have detected the SO_2 in the upper part of the boundary layer as well as near the ground, while the in situ monitor measured it only near the ground. This could cause inconsistency of SO_2 trends between the MAX-DOAS system and in situ monitor during the first event period. NO_2 levels in the boundary layer could be more affected by local sources near the measurement site than by the long-range transport during the event periods as NO_2 has relatively short lifetime compared to SO_2. It is believed that the majority of NO_2 measured during the event periods could be attributed to local sources such as increased traffic around nearby resorts rather than the long-ranged transport from Asian continent. This could be supported by higher NO concentration during the event periods, compared to other periods. Therefore, temporal variation between the MAX-DOAS and in situ monitor was relatively consistent for NO_2 during the measurement period.

In addition to the long-range transport of pollutants, local sources (e.g., increased traffic around nearby resorts on a weekend) could have contributed to the high concentrations of SO_2 and

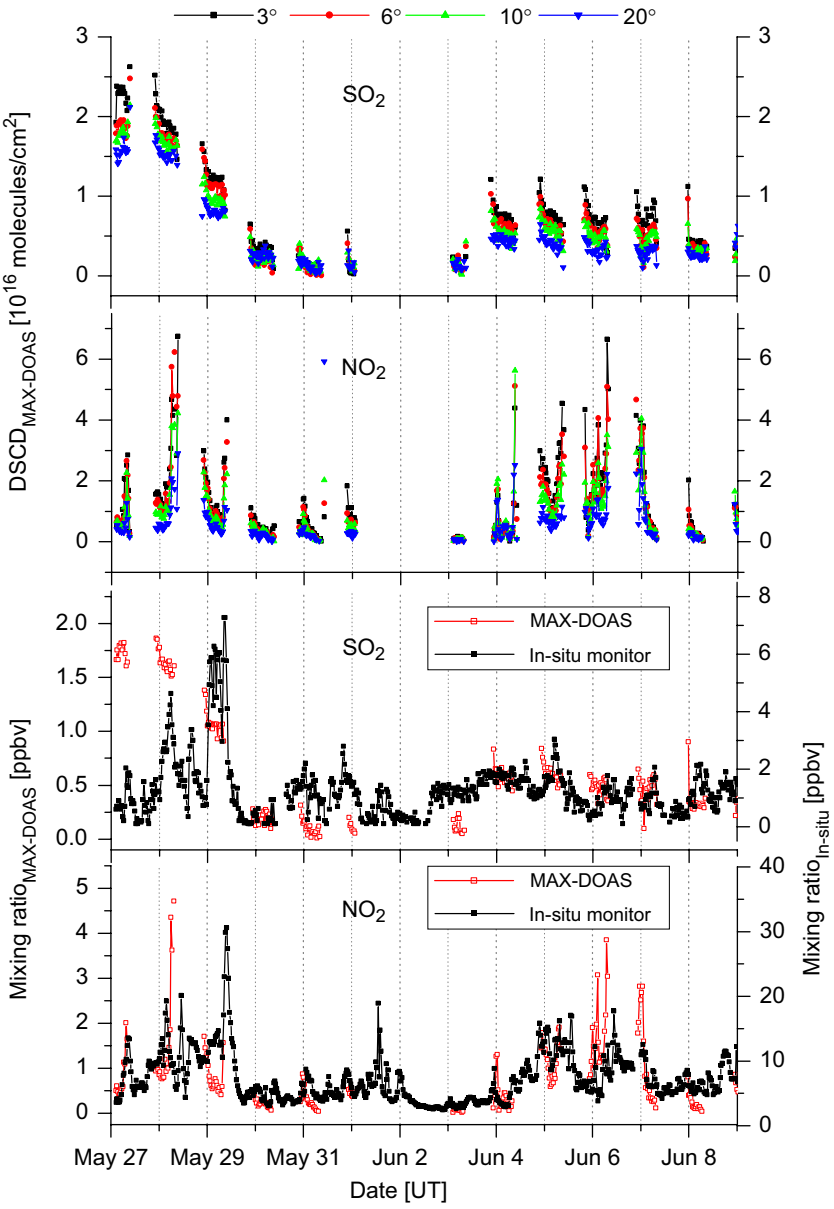

Fig. 1. Differential slant column densities (DSCD) and mixing ratios of SO_2 and NO_2 at different elevation angles (denoted on the top of the figure) determined by the MAX-DOAS system at KGAWO. Mixing ratios by the MAX-DOAS system were calculated using DSCD at the elevation angle 6° and a 1 km well-mixed boundary layer (for details see Section 3.1). The date at the tic-mark denotes 0:00 h (UT) of the given day.

NO_2 during the first event period, particularly on 29 May 2005. The increased concentrations of SO_2 and NO_2 observed during the second period on a weekend could be attributed to local sources.

The mean DSCDs of SO_2 and NO_2 observed during the measurement period can be converted to mixing ratios. Assuming that the trace gases were homogeneous within the 1 km height of the boundary mixing ratios were calculated as (Ziemke et al., 2001)

$$M\,(\mathrm{ppbv}) = 1.25 \times \frac{\mathrm{DSCD}\,(\mathrm{molecules\,cm^{-2}})}{\mathrm{dAMF}} \times \frac{1}{2.688 \times 10^{16}\,(\mathrm{molecules\,DU^{-1}})} \times \frac{1}{\Delta P\,(\mathrm{atom})}, \quad (1)$$

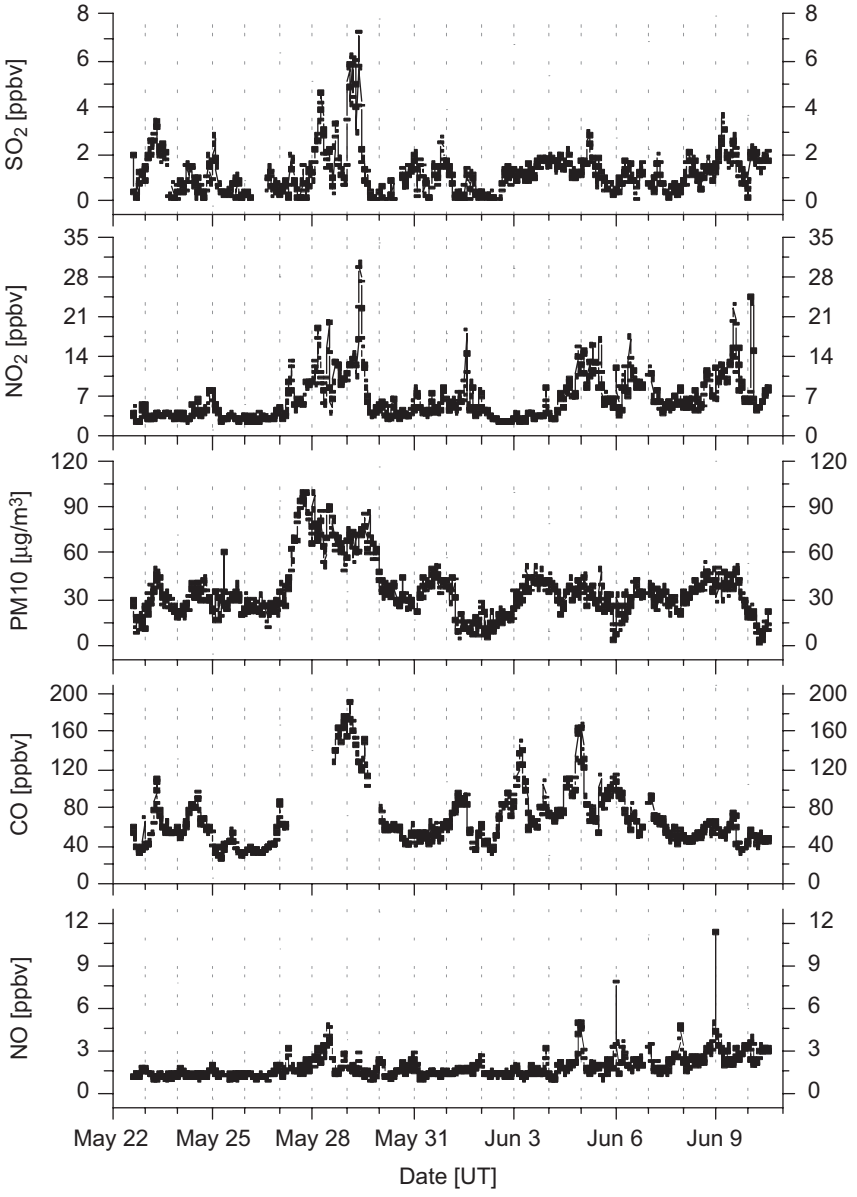

Fig. 2. Mixing ratios of SO_2, NO_2, PM_{10}, CO, and NO obtained by in situ monitors at KGAWO. The date at the tic-mark denotes 0:00 h (UT) of the given day.

Table 2
SO_4^{2-}/SO_2 ratios determined for each PM_1 sample collected for 24 h

	27 May	29 May	30 May	31 May	4 June	5 June	6 June	7 June	8 June
SO_4^{2-}/SO_2 ratio	6.05	1.36	5.98	0.82	1.37	0.76	1.77	1.41	2.74

where M is the mixing ratio, dAMF is a differential airmass factor (AMF($\alpha = 6^\circ$)–AMF($\alpha = 90^\circ$)), and ΔP is the pressure difference between surface and 1 km height of boundary layer, which was determined to be 0.113 from US standard atmosphere, 1976 (Seinfeld and Pandis, 1998). The AMFs for this work were calculated using the Monte Carlo radiative transfer model described in von

Friedeburg et al. (2004) which includes multiple Rayleigh and Mie scattering, surface albedo, refraction, and full spherical geometry. Assuming 30° solar zenith angles, 5% ground albedo, and trace gas profiles where the absorption was below 1 km in the boundary layer, the dAMFs were calculated to be 4.8 at 310 nm for SO_2 and 5.7 at 410 nm for NO_2, respectively, based on an aerosol profile measured by a collocated LIDAR instrument on 29 May (UT). The mixing ratios converted from DSCDs of SO_2 and NO_2 observed during the measurement period are shown in Fig. 1. Assuming that the trace gases were well mixed within the 1 km height of the boundary layer, the mean mixing ratios of SO_2 and NO_2 were estimated to be 0.62 ($\pm$0.60) ppbv and 0.80 ($\pm$0.77) ppbv, respectively.

The mixing ratios of SO_2 and NO_2 derived from the MAX-DOAS data are much lower compared to those obtained by the in situ monitors. The AMF for the calculation of SO_2 and NO_2 mixing ratios depends strongly on their vertical profiles (e.g., Hönninger et al., 2004; Richter et al., 2005, 2006). It is believed that a lot of SO_2 was above the boundary layer for the high SO_2 events. High SO_2 plume could be above the boundary layer on 27–29 May, and is already decreasing on 29 May when it was detected by the in situ monitor. There is some separation of viewing angles in the SO_2 during the measurement period indicating a boundary layer signal where the in situ sensor detects elevated SO_2. The plume could be on top of the boundary layer and did not lead to more separation but rather to an offset in all viewing directions. In the case of NO_2, the NO_2 is not well mixed in the boundary layer and therefore the mixing ratio at the surface is usually larger than what would be expected from an 1 km well-mixed layer.

Table 3 summarizes the statistical results of atmospheric NO_2, SO_2, CO, and PM_{10} concentrations determined by the in situ gas analyzers. The measurement period of 20 May to 10 June 2005 was divided into three periods with the events previously mentioned. Fig. 3 shows the meteorological parameters measured at KGAWO during the above period, indicating that wind was northerly or northwesterly during the event periods. A high-pressure system was located over the Northeast of China until 26 May 2005 and during the two events periods, and then low pressure settled in from 27 May to 2 June 2005. As in the cases of NO_2 and SO_2, relatively high CO and PM_{10} concentrations were observed during the first period, but not during the second event period in the case of PM_{10}. The CO concentration measured during the first event period was higher than that obtained during the second period, as shown in Table 3. During the first event period, the mean concentrations of CO and PM_{10} were 137.3 ± 36.4 ppmv and $68.2 \pm 16.8\ \mu g\ m^{-3}$, respectively.

3.2. Synoptic conditions and air-mass backward trajectories

Fig. 4 shows the mean sea-level pressure charts with wind vector at 850 hPa from 20 May to 10 June 2005. As shown in Fig. 4, the time series for mean sea-level pressure indicate that the continental high-pressure system was located over Northeastern China and the prevailing airflows in the rim regions was northerly or northwesterly during 21–26 May

Table 3
Measurement results of ground-based in situ air quality monitoring instruments during period of 21 May to 10 June 2005

	Case w/o the events[a]				1st event case				2nd event case			
	NO_2	SO_2	CO	PM_{10}	NO_2	SO_2	CO	PM_{10}	NO_2	SO_2	CO	PM_{10}
Mean	6.5	1.0	57.2	29.1	9.3	1.6	137.3	68.2	8.2	1.1	81.5	30.6
Std	3.1	0.8	19.7	11.3	4.6	1.6	36.4	16.8	3.4	0.6	25.8	8.4
Max	27.8	4.0	155.4	66.2	34.5	7.8	200.1	108.0	24.4	3.3	182.8	52.5
Min	2.3	0.0	25	0.0	3.2	0.0	57.4	23.8	2.9	0.0	41.9	1.4
Med	4.3	1	54	29.5	9.2	1.2	145.9	69.3	7.5	1.1	74.4	8.4
N	1728	1728	1728	1721	432	432	172	431	552	552	552	552

Mean, Std, Max, Min, Med, *N* denote the mean, standard deviation, maximum, minimum, median values, and the number of data for each case, respectively.

[a]The period of excluding the first event period (27–29 May) and the second period (4–7 June) from 20 May to 10 June 2005.

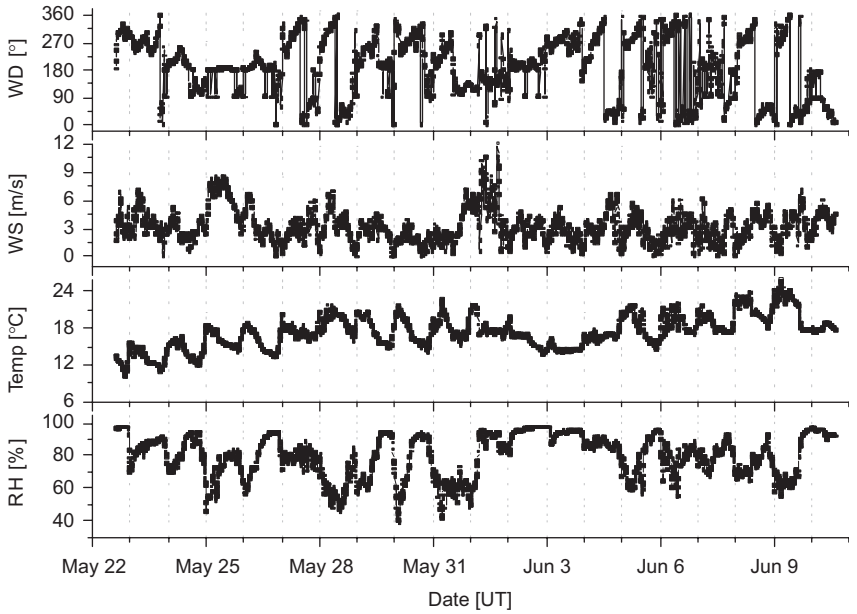

Fig. 3. Meteorological data collected by an automatic weather station installed 40 m above the ground level at KGAWO. WD, WS, Temp., and RH denote the wind direction, wind speed, temperature, and relative humidity, respectively.

2005. The wind was westerly or southwesterly during 27 May to 1 June, was northerly or northwesterly during 2–4 June, and then changed to be westerly or southwesterly from 7 June 2005. High SO_2 VCDs were observed around the Korean peninsula by SCIAMACHY during 21–26 May 2005 (see Section 3.3).

Air-mass backward trajectories were calculated to investigate the sources and pathway of air-masses reaching Korea. The NOAA/ARL HYSPLIT-4 model was used to calculate backward trajectories of air-masses with a 00 UTC (09:00 h local time) arrival time at Anmyeon, Korea. The 5-day (120 h) backward trajectories at three heights of 500, 1000, and 2000 m (above the ground level) are plotted in Fig. 5. The top and bottom graphs of air-mass trajectory analysis show the horizontal and vertical motion of an air-mass, respectively. As shown in Fig. 5, the trajectory lines show that the air-masses reaching Anmyeon passed over Northeast China and Korea at all altitudes. The trajectory results show that the air-mass from Mongolia moved to the southeast, and then it picked up the high SO_2 plume while passing over Chinese industrial areas (36–44°N and 114–124°E) and metropolitan areas (e.g., Beijing) of Northeast China, before arriving at Anmyeon. Vertical movement of the trajectory shows that the air-mass can be affected by emissions from Chinese industrial and metropolitan areas. In particular, backward trajectories for the altitudes of 500 and 1000 m passed through the industrial areas in China. The interesting results were that the air-mass for each altitude stayed in Northeast China for around 4 days and then reached Anmyeon, Korea.

3.3. Satellite images of SO_2

Fig. 6 shows the tropospheric vertical columns of SO_2, obtained from SCIAMACHY spectral data. The sub pixel gaps marked as white color in Fig. 6 were induced by cloud screening to remove those pixel data with a cloud fraction >0.6 as mentioned in Section 2.3. The SCIAMACHY scanned once per 3 days over Korea. The data focus on the period from 18 May to 10 June 2005. No significant SO_2 values were seen over the study area of around East China and the Korean peninsula during the period of 18–20 May. Enhanced SO_2 values were detected over industrial areas in Northeast China, around the Korean peninsula, and over West Sea around the longitude 124° during 21–23 May. SCIAMACHY SO_2 VCDs over these areas ranged up to 1.4×10^{17} mol cm^{-2}. From 24 to 26 May, these enhanced SO_2 values were detected around West Sea coast and East Sea (around 132°E and 40°N) and were as high as 1.3×10^{17} mol cm^{-2}. Note that

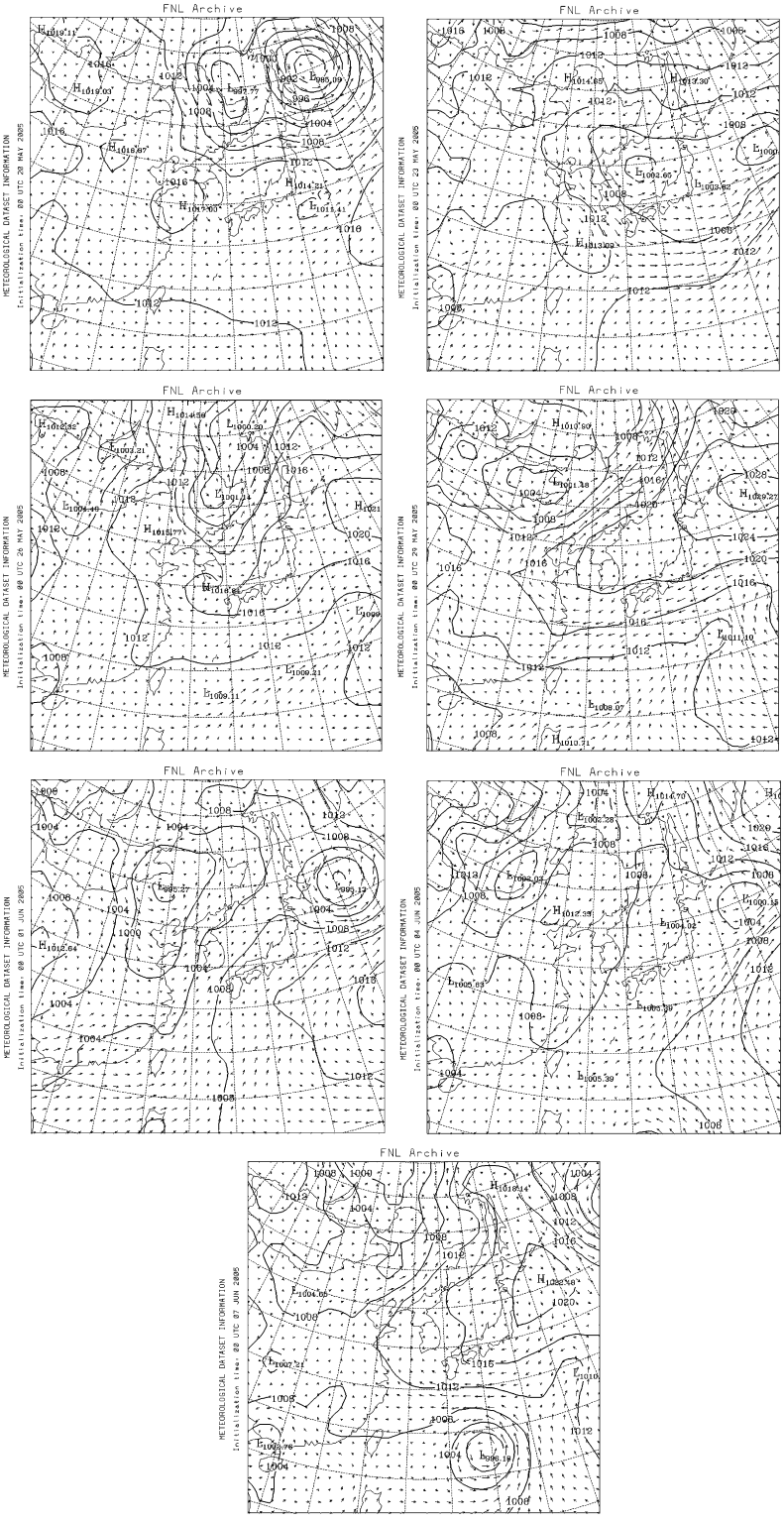

Fig. 4. Mean sea-level pressure charts with wind vector at 850 hPa over Northeast Asia for the period of 20 May to 10 June 2003 (UT). The mean sea-level pressure contour interval is 4 hPa. Meteorological data are from the NOAA/ARL FNL archive.

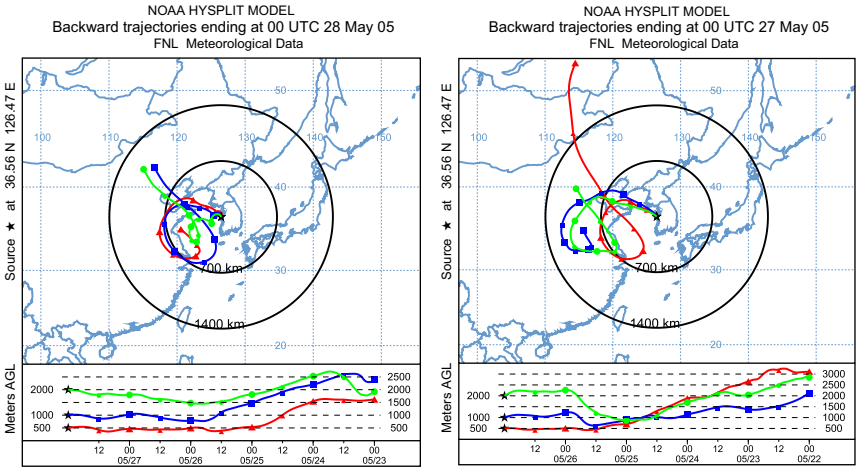

Fig. 5. HYSPLIT backward trajectories, indicating the origin of airmasses observed at KGAWO in May 2005: left, 27 May; right, 28 May. Asterisks indicate the start point of the backward trajectories; other marks along the trajectories are spaced 12 h apart. The bottom plots show the height (above the ground level) as functions of the time in h before the start of the trajectory.

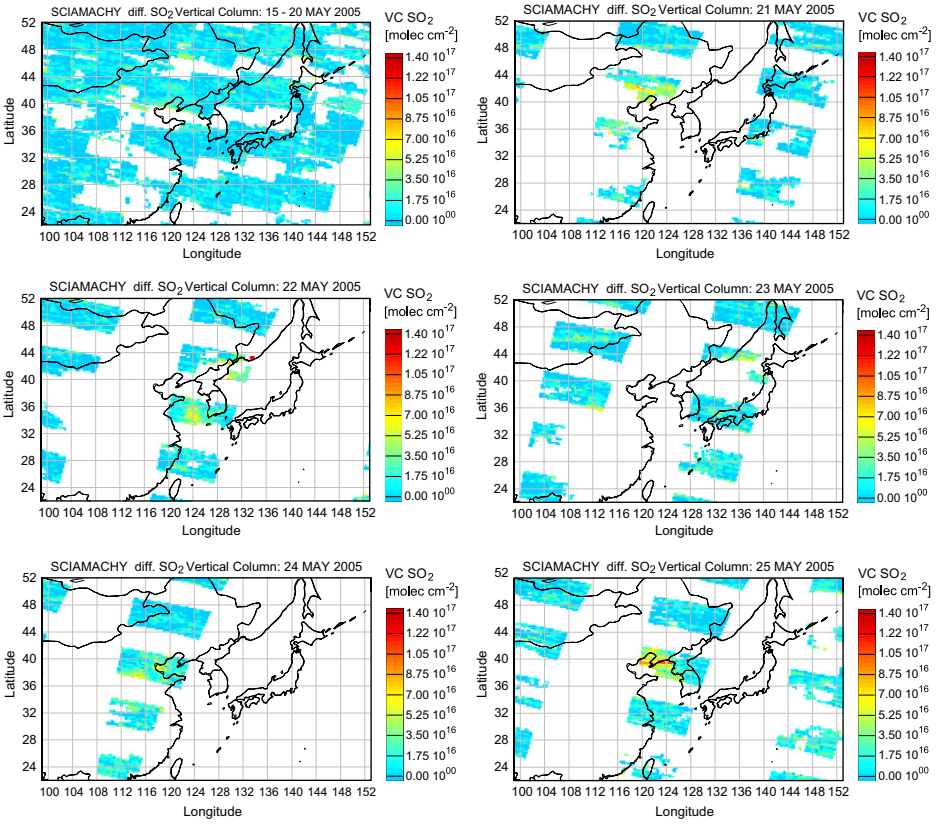

Fig. 6. Tropospheric SO_2 vertical columns from SCIAMACHY retrieval. The daily plots are shown in the period of 21–29 May 2005 of interest. The other plots are based on 6-day mean data.

there was no significant emission source of SO_2 in West Sea and East Sea. They could be the result of transport from the area where the high SO_2 plumes were detected during the period of 21–23 May since the wind was northwesterly around the Korean peninsula during this period (see Fig. 4). No

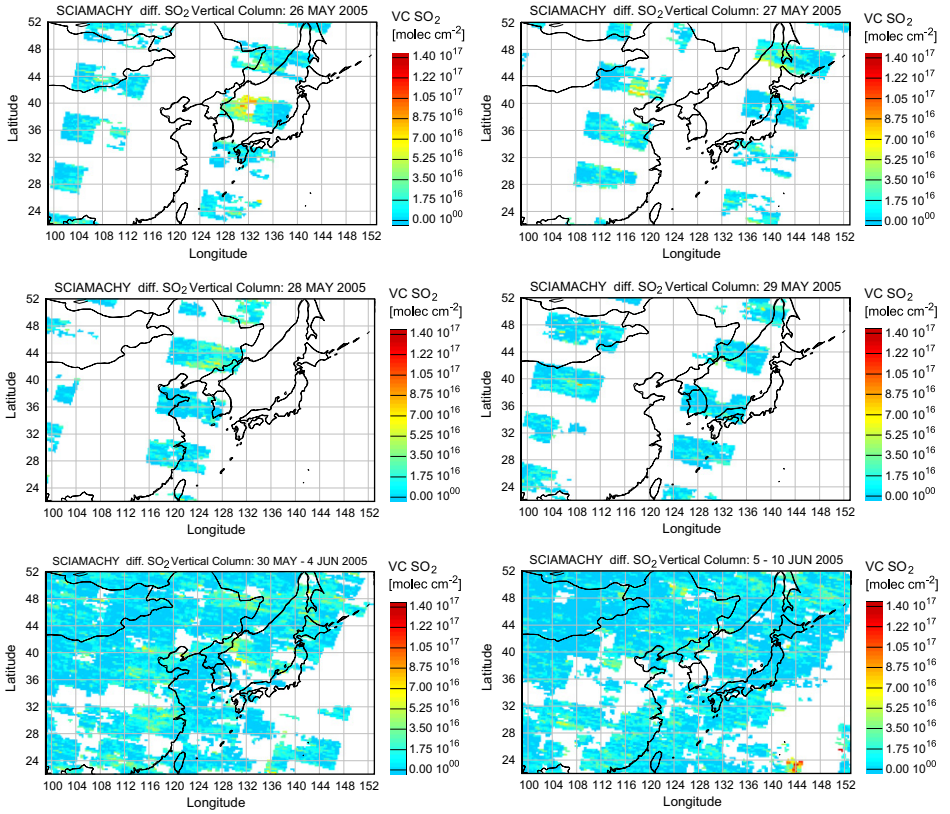

Fig. 6. (*Continued*)

significant SO_2 values were observed from 27 May to 10 June. However, the SO_2 values around the Korean peninsula slightly increased during the period of 1–7 June, and then decreased from 8 June. The maximum SO_2 columns were 7.0×10^{16} mol cm^{-2} around the Korean peninsula during the period of 27 May to 4 June. High SO_2 plumes have been observed over the area of latitude 22–24° and longitude 132–136° as shown in the first plot of Fig. 6. However, they did not have an effect on air quality over Korea during the measurement period because of the meteorological conditions as shown in Fig. 4.

The high SO_2 values from SCIAMACHY data were observed over Chinese industrial areas during the period of 21–25 May and over West Sea coast during the period of 22–26 May. As seen on the meteorological maps of Fig. 4, the wind was southeasterly and HYSPLIT-4 modeling results show the air-masses detected at KGAWO had passed over Chinese industrial areas where high SO_2 and low NO_2 were detected by SCIAMACHY during the period (b). During the period of 21–26 May relatively high NO_2 was observed over the West Sea, compared to other periods. The SO_2 VCD from the SCIAMACHY retrieval over Chinese industrial areas (36–44°N and 114–124°E) where the air-masses passed before arriving at Anmyeon was as high as 1.4×10^{17} mol cm^{-2}, and the SO_2 VCD integrated over these areas ($\int_x \int_y \mathrm{VCD}_{SO_2}(x,y)\,dx\,dy$) was $\sim 2.3 \times 10^{32}$ molecules ($\sim 2.4 \times 10^4$ SO_2 ton). The SO_2 VCD retrieved from SCIAMACHY data at KGAWO was 3.4×10^{15} mol cm^{-2} ($\sim$1.4 ppbv, assuming that the trace gases were well mixed within 1 km height of the boundary layer) on 28 May 2005. The mean SO_2 concentrations were 1.4 and 1.6 ppbv (ranged to 1.8 and 7.8 ppbv) by the MAX-DOAS system and an in situ gas analyzer, respectively, at KGAWO during the first event period.

High NO_2 columns were observed during the above measurement periods over East China (and also over Seoul located in the middle of the Korea peninsula), as shown in Fig. 7. Relatively high NO_2 was observed over the West Sea region during 21–26 May 2005, compared to other periods.

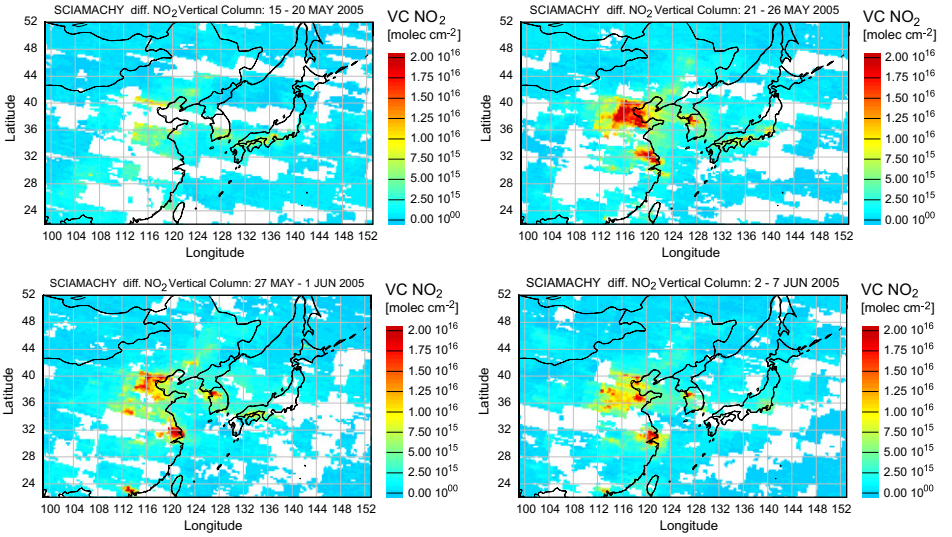

Fig. 7. Tropospheric NO_2 vertical columns from SCIAMACHY retrieval. The plots are based on 6-day mean data from 15 May to 7 July 2005.

4. Conclusions

Atmospheric pollutants (in particular SO_2) originating from the Asian continent were transported to the Korean peninsula during May 2005, with the movement of these air-masses being dependent on synoptic weather conditions. Trajectory calculations show that the air-masses passed over the Chinese industrial areas and picked up the high SO_2 plumes, before arriving at KGAWO (the ground-based measurement site). The tropospheric SO_2 VCDs over these Chinese industrial areas ranged to 1.4×10^{17} mol cm^{-2} in SCIAMACHY data. The SO_2 plume originating from the Asian continent extended far to the Southeast over Korea and moved out to the East Sea. Relatively high SO_2 levels were observed by the ground-based MAX-DOAS system over the KGAWO site during 27–29 May 2005 and ranged to 2.5×10^{16} and 6.2×10^{16} DSCD mol cm^{-2} at the elevation angle 6°. Mean surface SO_2 values measured at the KGAWO site by the in situ gas analyzer ranged to 7.8 ppbv, which was highly affected by SO_2 plumes originating from Chinese industrial and metropolitan areas. The atmospheric trace gases transported from the Asian continent could have impact on the regional air quality over Korea. The estimation of anthropogenic trace gas emissions and their transport from space have difficulties due to inadequate coverage of satellite data in time and space. However, the satellite remote sensing techniques can help investigate the extent of long-range transport of anthropogenic trace gases and their impact on local air quality, complementing ground-based measurement.

Acknowledgments

This work was supported by the Korea Research Foundation Grant funded by the Korean Government (MOEHRD) (KRF-2006-214-D00085), and by the Korea Science and Engineering Foundation through the Advanced Environmental Monitoring Research Center (ADEMRC) at Gwangju Institute of Science and Technology (GIST). The SCIAMACHY data were obtained from Institute of Environmental Physics and Remote Sensing, University of Bremen, Germany. The Software package of WinDOAS for evaluation of MAX-DOAS spectra was offered from Belgium Institute for Space Aeronomy, Belgium. The TRACY software package for the AMF calculation was given from Institute of Environmental Physics, University of Heidelberg, Germany.

References

Afe, O.T., Richter, A., Sierk, B., Wittrock, F., Burrows, J.P., 2004. BrO emission from volcanoes: a survey using GOME and SCIAMACHY measurements. Geophysical Research Letters 31, doi:10.1029/2004GL020994.

Aliwell, S.R., van Roozendael, M., Johnston, P.V., Richter, A., Wagner, T., Arlander, D.W., Burrows, J.P., Fish, D.J., Jones, R.L., Tørnkvist, K.K., Lambert, J.C., Pfeilsticker, K., Pundt, I., 2002. Analysis for BrO in zenith-sky spectra: an intercomparison exercise for analysis improvement. Journal of Geophysical Research 107, doi:10.1029/2001JD000329.

Berglen, T.F., Berntsen, T.K., Isaksen, I.S.A., Sundet, J.K., 2004. A global model of the coupled sulfur/oxidant chemistry in the troposphere: the sulfur cycle. Journal of Geophysical Research 109, doi:10.1029/2003JD003948.

Bobrowski, N., Hönninger, G., Galle, B., Platt, U., 2003. Detection of bromine monoxide in a volcanic plume. Nature 423, 273–276.

Bogumil, K., Orphal, J., Homann, T., Voigt, S., Spietz, P., Fleischmann, O.C., Vogel, A., Hartmann, M., Bovensmann, H., Frerik, J., Burrows, J.P., 2003. Measurements of molecular absorption spectra with the SCIAMACHY pre-flight model: instrument characterization and reference data for atmospheric remote sensing in the 230–2380 nm region. Journal of Photochemistry and Photobiology A 157, 167–184.

Bovensmann, H., Burrows, J.P., Buchwitz, M., Frerick, J., Noel, S., Rozanov, V.V., Chance, K.V., Goede, A.H.P., 1999. SCIAMACHY-Mission objectives and measurement modes. Journal of Atmospheric Sciences 56, 127–150.

Buchwitz, M., de Beek, R., Burrows, J.P., Bovensmann, H., Warneke, T., Notholt, J., Meirink, J.F., Goede, A.P.H., Bergamaschi, P., Körner, S., Heimann, M., Schulz, A., 2005. Atmospheric methane and carbon dioxide from SCIAMACHY satellite data: initial comparison with chemistry and transport models. Atmospheric Chemistry and Physics 5, 941–962.

Chance, K., 1998. Analysis of BrO measurements from the Global Ozone Monitoring Experiment. Geophysical Research Letters 25, 3335–3338.

Chin, M., Jacob, D.J., 1996. Anthropogenic and natural contributions to tropospheric sulfate: a global model analysis. Journal of Geophysical Research 101, 18669–18691.

Chin, M., Savoie, D.L., Huebert, B.J., Bandy, A.R., Thornton, D.C., Bates, T.S., Quinn, P.K., Saltzmann, E.S., De Bruyn, W.J., 2000. Atmospheric sulfur cycle simulated in the global model GOCART: comparison with field observations and regional budgets. Journal of Geophysical Research 105, 24689–24712.

Eisinger, M., Burrows, J.P., 1998. Tropospheric sulfur dioxide observed by the ERS-2 GOME instrument. Geophysical Research Letters 25, 4177–4180.

Greenblatt, G.D., Orlando, J.J., Burkholder, J.B., Ravishankara, A.R., 1990. Absorption measurements of oxygen between 330 and 1140 nm. Journal of Geophysical Research 95, 18577–18582.

Guttikunda, S.K., Tang, Y., Carmichael, G.R., Kurata, G., Pan, L., Streets, D.G., Woo, J.-H., Thongboonchoo, N., Fried, A., 2005. Impacts of Asian megacity emissions on regional air quality during spring 2001. Journal of Geophysical Research 110, doi:10.1029/2004JD004921.

Hausmann, M., Platt, U., 1994. Spectroscopic measurement of bromine oxide and ozone in the high Arctic during Polar Sunrise Experiments 1992. Journal of Geophysical Research 99, 25399–25413.

Hebestreit, K., Stutz, J., Rosen, D., Matveiv, V., Pelg, M., Luria, M., Platt, U., 1999. DOAS measurements of tropospheric bromine oxide in mid-latitudes. Science 283, 55–57.

Hönninger, G., von Friedeburg, C., Platt, U., 2004. Multi-axis differential optical absorption spectroscopy (MAX-DOAS). Atmospheric Chemistry and Physics 4, 231–254.

Jaffe, D., Prestbo, E., Swartzendruber, P., Weiss-Penzias, P., Kato, S., Takami, A., Hatakeyama, S., Kajii, Y., 2005. Export of atmospheric mercury from Asia. Atmospheric Environment 39, 3029–3038.

Kokhanovsky, A.A., von Hoyningen-Huene, W., Rozanov, V.V., Noël, S., Gerilowski, K., Bovensmann, H., Bramstedt, M., Buchwitz, M., Burrows, J.P., 2006. The semianalytical cloud retrieval algorithm for SCIAMACHY II. The application to MERIS and SCIAMACHY data. Atmospheric Chemistry and Physics 6, 4129–4136.

Koike, M., Kondo, Y., Kita, K., Takegawa, N., Masui, Y., Miyazaki, Y., Ko, M.W., Weinheimer, A.J., Flocke, F., Weber, R.J., Thornton, D.C., Sachse, G.W., Vay, S.A., Blake, D.R., Streets, D.G., Eisele, F.L., Sandholm, S.T., Singh, H.B., Talbot, R.W., 2003. Export of anthropogenic reactive nitrogen and sulfur compounds from the East Asia region in spring. Journal of Geophysical Research 108, doi:10.1029/2002JD003284.

Lee, C., Choi, Y.J., Jung, J.S., Lee, J.S., Kim, Y.J., Kim, K.H., 2005a. Measurement of atmospheric monoaromatic hydrocarbons using differential optical absorption spectroscopy: comparison with on-line gas chromatography measurements in urban air. Atmospheric Environment 39, 2225–2234.

Lee, C., Kim, Y.J., Tanimoto, H., Bobrowski, N., Platt, U., Mori, T., Yamamoto, K., Hong, C.S., 2005b. High ClO and ozone depletion observed in the plume of Sakurajima volcano. Geophysical Research Letters 32, doi:10.1029/2005GL023785.

Leser, H., Hönninger, G., Platt, U., 2003. MAX-DOAS measurements of BrO and NO_2 in the marine boundary layer. Geophysical Research Letters 30, doi:10.1029/2002GL015811.

Myhre, G., Berglen, T.F., Myhre, C.E.L., Isaksen, I.S.A., 2004. The radiative effect of the anthropogenic influence on the stratospheric sulfate aerosol layer. Tellus B 56, doi:10.1111/j.1600-0889.2004.00106.x.

Palmer, P.I., Jacob, D.J., Fiore, A.M., Martin, R.V., Chance, K., Kurosu, T.P., 2003. Mapping isoprene emissions over North America using formaldehyde column observations from space. Journal of Geophysical Research 108, doi:10.1029/2002JD002153.

Platt, U., 1994. Differential optical absorption spectroscopy (DOAS). In: Sigrist, M.W. (Ed.), Monitoring by Spectroscopic Techniques. Wiley, New York, pp. 27–84.

Richter, A., Burrows, J.P., 1999. Tropospheric NO_2 from GOME measurements. Advanced Space Research 29, 1673–1683.

Richter, A., Burrows, J.P., Nüß, H., Granier, C., Niemeier, U., 2005. Increase in tropospheric nitrogen dioxide over China observed from space. Nature 437, 129–132.

Richter, A., Wittrock, F., Burrows, J.P., 2006. SO_2 Measurements with SCIAMACHY, DPG Frühjahrstagung, March 2006.

Seinfeld, Pandis, 1998. Atmospheric Chemistry and Physics. Wiley, New York, USA.

Sierk, B., Richter, A., Rozanov, A., von Savigny, Ch., Schmoltner, M., Buchwitz, M., Bovensmann, H., Burrows, J.P., 2006. Retrieval and monitoring of atmospheric trace gas concentrations in nadir and limb geometry using the space-borne SCIAMACHY instrument. Environmental Monitoring and Assessment, doi:10.1007/s10661-005-9049-9.

Simon, F.G., Schneider, W., Moortgat, G.K., Burrows, J.P., 1990. A study of the ClO absorption cross-section between 240 and 310 nm and the kinetics of the self-reaction at 300 K. Journal of Photochemistry and Photobiology A: Chemistry 55, 1–23.

Stohl, A., Huntrieser, H., Richter, A., Beirle, S., Cooper, O.R., Eckhardt, S., Forster, C., James, P., Spichtinger, N., Wenig, M., Wagner, T., Burrows, J.P., Platt, U., 2003. Rapid intercontinental air pollution transport associated with a meteorological bomb. Atmospheric Chemistry and Physics 3, 969–985.

Stutz, J., Platt, U., 1996. Numerical analysis and error estimation of differential optical absorption spectroscopy measurements least-squares methods. Applied Optics 35, 6041–6053.

Tan, Q., Huang, Y., Chameides, W.L., 2002. Budget and export of anthropogenic SO_x from East Asia during continental outflow condition, Journal of Geophysical Research 107, doi:10.1029/2001JD000769.

Tu, F.H., Thornton, D.C., Bandy, A.R., Carmichael, G.R., Tang, Y., Thornhill, K.L., Sachse, G.W., Blake, D.R., 2004. Long-range transport of sulfur dioxide in the central Pacific. Journal of Geophysical Research 109, doi:10.1029/2003JD004309.

Vandaele, A.C., Simon, P.C., Guilmot, J.M., Carleer, M., Colin, R., 1994. SO_2 absorption cross section measurement in the UV using a Fourier transform spectrometer. Journal of Geophysical Research 99, 25,599–25,605.

Vandaele, A.C., Hermans, C., Simon, P.C., Carleer, M., Colin, R., Fally, S., Mérienne, M.-F., Jenouvrier, A., Coquart, B., 1997. Measurements of the NO_2 absorption cross-section from 42,000 to 10,000 cm^{-1} (238–1000 nm) at 220 and 294 K. Journal of Quantitative Spectroscopy and Radiative Transfer 59, 171–184.

Van Roozendael, M., Fayt, C., 2001. WinDOAS 2.1 Software User Mannual, Uccle, IASB/BIRA.

von Friedeburg, C., Wagner, T., Geyer, A., Kaiser, N., Vogel, B., Vogel, H., Platt, U., 2004. Derivation of tropospheric NO_3 profiles using off-axis differential optical absorption spectroscopy measurements during sunrise and comparison with simulations. Journal of Geophysical Research 107, doi:10.1029/2001JD000481.

Vountas, M., Rozanov, V.V., Burrows, J.P., 1998. Ring effect: impact of rotational Raman scattering on radiative transfer in earth's atmosphere. Journal of Quantitative Spectroscopy and Radiative Transfer 60, 943–961.

Wagner, T., Platt, U., 1998. Satellite mapping of enhanced BrO concentrations in the troposphere. Nature 395, 486–490.

Wilmouth, D.M., Hanisco, T.F., Donahue, N.M., Anderson, J.G., 1999. Fourier transfer ultraviolet spectroscopy of the A2P3/2 X2P3/2 transition of BrO. Journal of Physical Chemistry A 103, 8935–8945.

Wittrock, F., Richter, A., Oetjen, H., Burrows, J.P., Kanakidou, M., Myriokefalitakis, S., Volkamer, R., Beirle, S., Platt, U., Wagner, T., 2006. Simultaneous global observations of glyoxal and formaldehyde from space. Geophysical Research Letters 33, doi:10.1029/2006GL026310.

Zhang, X.Y., Gong, S.L., Shen, Z.X., Mei, F.M., Xi, X.X., Liu, L.C., Zhou, Z.J., Wang, D., Wang, Y.Q., Cheng, Y., 2003. Characterization of soil dust aerosol in China and its transport and distribution during 2001 ACE-Asia: 1. Network observations. Journal of Geophysical Research 108, doi:10.1029/2002JD002632.

Ziemke, J.R., Chandra, S., Bhartia, P.K., 2001. Cloud slicing: a new technique to derive upper tropospheric ozone from satellite measurements. Journal of Geophysical Research 106, 9853–9867.